University of Huddersfield Repository

Li, Guoxing, Gu, Fengshou, Wang, Tie, Yang, Tiantian and Ball, Andrew

Investigation into the dynamic response of cylinder liners in an IC engine based on a validated finite-element model

Original Citation

Li, Guoxing, Gu, Fengshou, Wang, Tie, Yang, Tiantian and Ball, Andrew (2017) Investigation into the dynamic response of cylinder liners in an IC engine based on a validated finite-element model. Systems Science & Control Engineering, 5 (1). pp. 56-69. ISSN 2164-2583
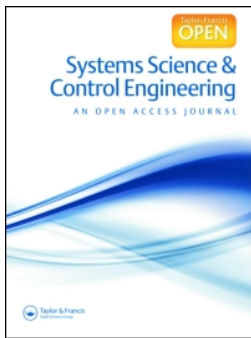
This version is available at http://eprints.hud.ac.uk/id/eprint/32005/

http://eprints.hud.ac.uk/

Investigation into the dynamic response of cylinder liners in an IC engine based on a validated finite-element model

Guoxing Li, Fengshou Gu, Tie Wang, Tiantian Yang & Andrew Ball

Published online: 19 Jan 2017.

Submit your article to this journal ⚲

Article views: 174

View related articles ⚲

View Crossmark data ⚲

Taylor & Francis
Taylor & Francis Group

ᵔ OPEN ACCESS

Investigation into the dynamic response of cylinder liners in an IC engine based on a validated finite-element model

Guoxing Li[a,b], Fengshou Gu[a,b], Tie Wang[a], Tiantian Yang[a] and Andrew Ball[b]

[a]Department of Vehicle Engineering, Taiyuan University of Technology, Taiyuan, People's Republic of China; [b]Centre for Efficiency and Performance Engineering, University of Huddersfield, Huddersfield, UK

ABSTRACT

To understand the effects of vibration of cylinder liners on engine combustion performance, tribological behaviour and vibro-acoustic radiations, this study investigates the dynamic responses of cylinder liners by finite-element modelling and experimental validation. The finite-element model is established in this study to predict the dynamic responses of cylinder liners to two significant sources: combustion shock and piston side thrust. It takes into account both the characteristics of structural modes and nonlinearities of assembly constraints when selecting adequate elements for efficient computation of the responses under both the highly nonlinear combustion pressure excitations and subsequent piston slap impacts. The predictions are then evaluated against experimental results under different engine operating conditions. To suppressing noise in measured signals, continuous wavelet analysis is employed to process the complicated responses for characterizing key response events and their frequency ranges. The results show agreeable correspondences between the numerical predictions and measured vibration signals, paving the way for investigating its effect on the combustion and lubrication processes.

1. Introduction

Compression ignition method of diesel engines results in higher in-cylinder pressure and higher efficiency, but also results in increased engine vibration and noise due to faster cylinder pressure rise, compared to gasoline engines. Due to the lack of physical model-based systematic research, a deep understanding of the generating mechanism and response characteristics of diesel engines' vibration and noise emissions has not been achieved. To investigate the response characteristics of engine vibrational responses to different excitation sources, it is essential to analyse the generating mechanism of dynamic behaviours based on an accurate dynamic model.

The piston assembly is one of engine's subsystems that determine the performances of friction, lubrication, noise, vibration and hence service lifespan. Previous studies showed that over 80% of the total engine vibration and noise emissions can be attributed to the dynamic response of cylinder liners under the excitation of the in-cylinder combustion and its consequent piston slaps (Hiroshi, Okubo, & Yonezawa, 1990). Moreover, this high fraction of vibration implies that dynamic interactions are rather intensive among mixture combustions,

hydrodynamic lubrication and liner dynamics. Therefore, active research has been carried out in order to understand and improve the dynamic behaviours of cylinder liners.

The difficulty in studying liner dynamics is to understand how to identify and locate the correspondence between the complex dynamic response and different excitation sources. Many researchers have focused on the identification and extraction of characteristic signals by using advanced signal analysis techniques. Geng and Chen (2005) used wavelet decomposition and a fast reconstruction algorithm to implement the impact-source separation. Liu and Randall (2005) introduced another identification method, that is, the blind source separation (BSS) for the separation of engine piston slaps from other vibration events. Badaoui, Danière, Guillet, and Servière (2005) and Servière, Lacoume, and El Badaoui (2005) compared Wiener filtering and BSS techniques to separate mechanical events and combustion noises. These studies have yielded some practical results of feature signal identification and extraction.

However, in the absence of a deep understanding of vibration generation mechanism, the signal identification only by using numerical analysis method is difficult to

---

implement, and even lead to erroneous conclusions. It is essential to make a thorough and detailed study on the dynamic behaviours of cylinder liners. Geng and Chen (2005) and Dolatabadi, Theodossiades, and Rothberg (2015) studied the dynamic response of cylinder liners by establishing mathematical dynamic model and proposed preliminary predictions about the occurrence timing and observable numbers of piston slaps on liners. Nonetheless, due to the limited degree of freedom (DOF), difficulty of defining boundary conditions and lack of structural characteristics, their predicted occurrence timing and observable number are not in good agreement with the experimental results. In order to obtain more accurate and reliable simulation results, some researchers investigated the liner dynamics by using the finite-element analysis (FEA) technique.

Structural analysis of cylinder liners has been reported using FEA (Cho & Moon, 2005; Jafari, Khalili, & Azarafza, 2005; Murakami, Nakanishi, Ono, & Kawano, 2011). The static deformation, forced response analysis and frequency response analysis of cylinder liners were undertaken based on finite-element models (FEMs), for impact force calculation and liner response analysis (Murakami et al., 2011). However, the majority of these FEM-based studies were performed based on a quasi-static model which the modal characteristics and reaction upon piston of cylinder liners were neglected. Obviously, such models may not be able to reflect the phenomena of true contacts between piston and cylinder due to invertible elastic deformations under dynamic forces.

Compared to shell elements, solid elements can better describe the geometric details of liner flanges, to facilitate the modelling of more realistic boundary conditions, although it comes at the cost of longer solution time (Jafari et al., 2005). To enhance the computing efficiency, Jafari et al. (2005) derived the dynamic response of cylindrical shells using the mode superposition method, which is recognized as the most powerful method to solve the equation sets of linear system considering the required solution time. The contact constraint widely existed in cylinder assembly is a typical nonlinear kinematic pair that cannot be handled by the mode superposition method (Wang & Nelson, 2002). To compensate, based on a direct Newmark integration method, Murakami et al. (2011) implemented the structure analysis of piston-cylinder assembly, coupling with multi-body dynamics analysis. However, due to excessive requirement for computational sources, numerical prediction of cylinder dynamic responses containing modal frequencies has not yet been achieved.

To gain an in-depth understanding of the dynamic responses of cylinder liners to in-cylinder combustion shocks and piston slaps, a finite-element dynamic model was established in this chapter, which takes into account both structural modal characteristics, nonlinearities of assembly constraints and time-varying exciting forces.

2. Establishment of finite-element model of cylinder assembly

Cylinder liners, also known as cylinder sleeves, are the central components of a reciprocating engine. Figure 1 shows a typical construction of the cylinder liner. The upper flange of cylinder liner is connected to the cylinder head and body through bolts, thus limiting its axial DOF. Both the upper and bottom external surfaces of liner are mounted onto the block within clearance fitting. To prevent leakage of liquid coolant into the crankcase, the lower end of the wet liner is sealed with the help of rubber sealing ring rather than being forced constraint with the engine block. It undertakes not only harsh combustion shocks but also strong piston slaps, which can affect tribological behaviour and oil consumption while it contributes significantly to engine vibration and noise emissions.

2.1. Meshing and solution algorithm

Under the preload of the cylinder-head bolts, the upper flange of cylinder liner is pressed against the cylinder block by cylinder head, as shown in Figure 2(a). The geometric details, especially the thickness, of the liner flange have a significant effect on the response characteristics of constraint modes of liner structure, and hence should not be over-simplified. Compared with shell elements, solid elements can better describe the geometric details of liner flanges in achieving a more realistic boundary
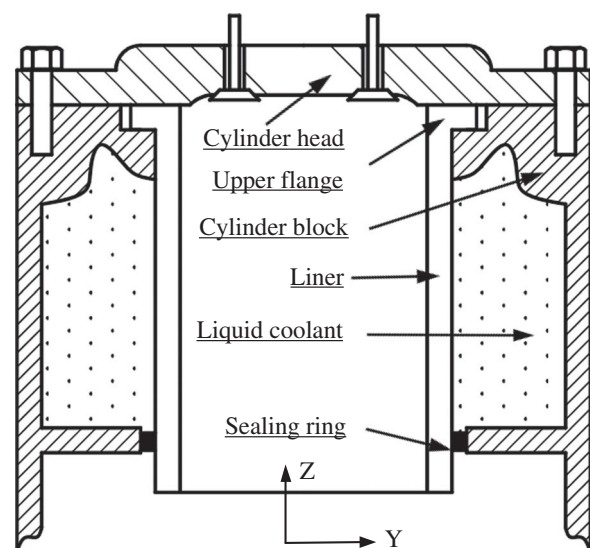

Figure 1. Construction of wet cylinder liner.
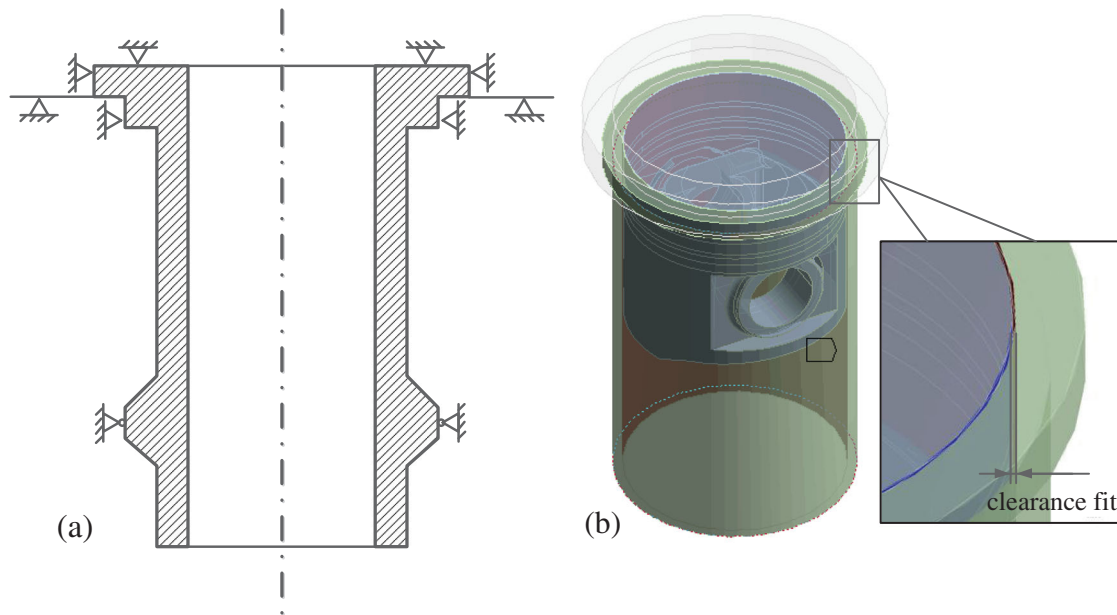
(a)

(b)

clearance fit

Figure 2. Boundary constraints of cylinder liner.

condition, although it comes at the cost of longer solution time. Because of the large number of simulation steps in the transient dynamics analysis, about 1000 steps for each case, both the larger number of grids and smaller mesh size can result in a dramatic increase in the need for solution time and computing sources. For the balance between better accuracy and efficiency, hexahedral elements with a grid size of 5 mm are adopted for three-dimensional meshes. To obtain the localized instantaneous deformations on the flanges at top end and the overall cylindrical shell, the model was configured to have 7121 hexahedral isoparametric solid elements using ANSYS Workbench. This finer element mesh arrangement is also taken into account that the vibration can have frequency contents as high as 10 kHz which was estimated based on analytic analysis when the liner is assumed to be an uniform cylindrical shell (Farshidianfar, Farshidianfar, Crocker, & Smith, 2011). To reduce the need for solution time and computing sources, all components other than the cylinder liner were treated as rigid body in modelling. Even so, the solution time required for the dynamic simulation of a whole operating cycle takes up to seven hours.

For dynamic simulations, modal superposition method is the most powerful method to solve the set of equations considering the required solution time. But, this method cannot handle the nonlinearities when the contact constraint is applied to the cylinder assembly (Wang & Nelson, 2002). Thus, the Newmark implicit integration method was used to solve nonlinear model in the cylinder dynamic simulation. To improve the computing efficiency, the reduced method, one subclass of Newmark

implicit integration method, was adopted to solve the motion equations of dynamic process.

2.2. Material and boundary conditions

Wet liners, or sleeves, are widely used in heavy-duty diesel engines, which allow engines to undertake high combustion loads without overheating because the coolant is in direct contact with the sleeve. A wet sleeve is essentially a standalone cylinder, supported at the top and bottom by the block, and surrounded by the water jacket.

In Figure 2(a), it shows the boundary conditions of a cylinder liner, being a non-uniform cylindrical shell and end-flanged cylindrical shell structure. To avoid changing modal characteristics of the cylinder liner caused by improper extra-constraints, the modelling of fixed joints and clearance fits has not been achieved by constraining the DOF, but through constructing a series of frictionless contact pairs, as given in Figure 2(b), which avoid the errors induced by over-simplification and inappropriate mathematical equivalent in the modelling and analysis of cylinder dynamic process (Farshidianfar et al., 2011). By defining boundary conditions in this way, slight changes in modal characteristics of the cylinder liner, induced by variations in local constraint status as the result of the dynamic deformation of matched surfaces, can be more accurately taken into account in the simulation.

The cylinder liner studied in this research was made of ductile cast iron QT600-3 ('ISO 1083', n.d.). The parameters for this material are listed in Table 1.

Table 1. Material properties of QT600-3.

Density (kg/m^{-3})	Young's modulus (Pa)	Poisson's ratio	Bulk modulus (Pa)	Shear modulus (Pa)
7120	1.69e+11	0.286	1.316e+11	6.5708e+10

2.3. Excitation configurations

Axial movement of the piston is controlled by the crankshaft and connecting rod mechanism. The driving force for piston lateral movement is defined by the side-thrust force calculated in Section 3 and Equation (1). The last one translational DOF of piston, which is perpendicular to the moving plane, is set as free to avoid over-constraint, as shown in Figure 3(a). To simplify the calculation, besides the rotational DOF along the piston tilting motion is set as free, all the other rotational freedoms of piston are ignored.

The pressure data from the in-cylinder pressure sensor were taken as the combustion excitation. Theoretically, the instantaneous pressure value needs to be applied to the cylinder liner uniformly and dynamically at each time interval (crank angle) in order to obtain the full responses of the linear for an entire engine cycle. However, considering much higher pressure rise rate (PRR) in the combustion process, only the pressure amplitudes are applied corresponding to the major combustion duration which is around combustion top dead center (TDC)

and varying with combustion conditions due to different operating conditions. To speed up the simulation process, only 1800 sampling points were calculated to show the compression and power strokes, which was resampled from 3600 points of the raw cylinder pressure signal using a polyphase implementation. And the force applying zone was equivalently confined to the top zone of liner inside surface, as shown in Figure 3(b). The zone has a height of 15 mm, being allowed to simulate the effective contacting areas at the moment when the combustion shock occurs.

2.4. Calibration of finite-element model

To verify and calibrate simulation parameters of the FEM, a modal test was conducted to obtain the free-free modal responses of the liner. Then modal frequencies from both the modal test and FEA are compared to confirm the accuracy of the FE modelling.

As shown in the Table 2, the simulated modal frequencies agree well with the measured ones, with an error less than 3% except the first mode. This shows that the configuration of material parameters and simplified geometric shape are appropriate for the modelling, and sufficient to represent and characterize the dynamic response features of cylinder liner under 10 kHz. The first four mode shapes of cylinder liner are given in Table 3. It
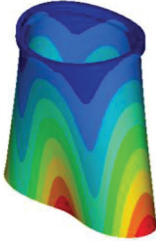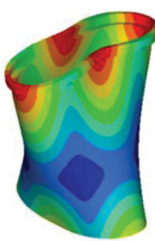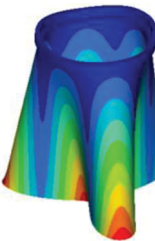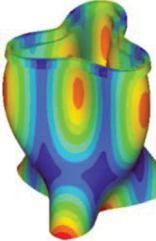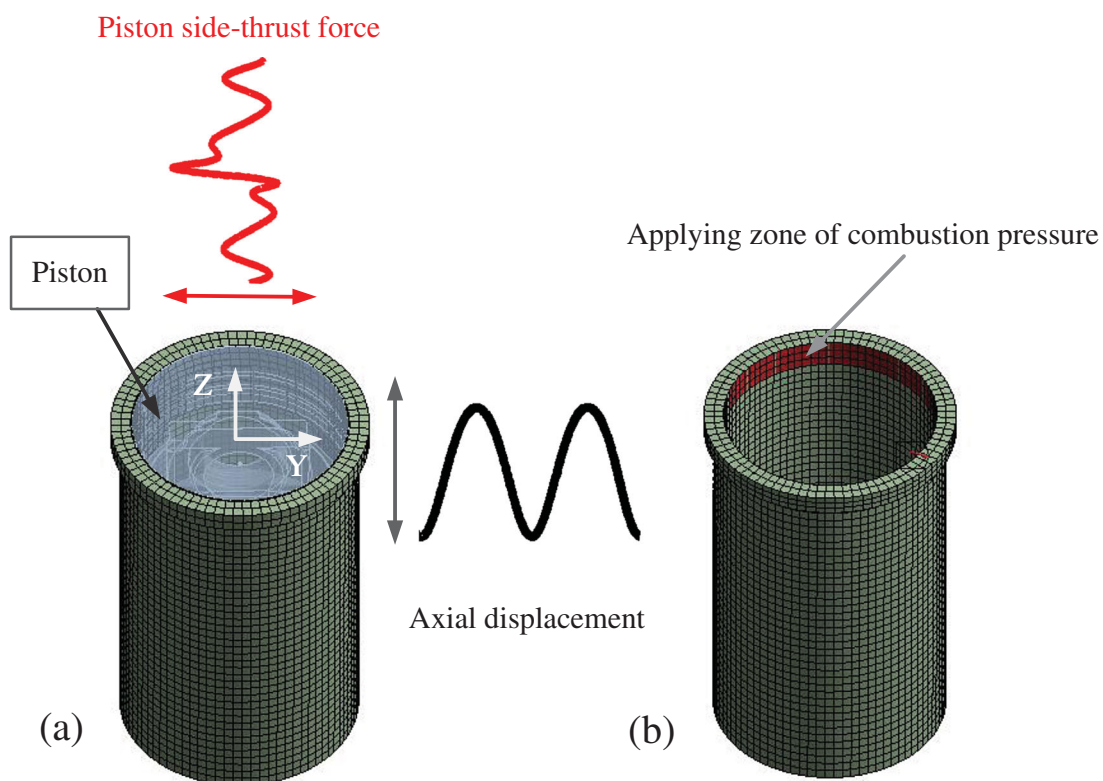

Figure 3. Excitation configurations of cylinder model.

Table 2. Simulated and measured mode frequencies of cylinder liner.

No.	Simulated Freq.(Hz)	Measured Freq.(Hz)	Error (%)	No.	Simulated Freq.(Hz)	Measured Freq.(Hz)	Error (%)
1	929.0	974.7	4.62	9	6673.2	6569.7	1.58
2	1229.7	1217.5	1.04	10	6979.5	6896.1	1.21
3	2567.3	2584.8	0.68	11	7926.9	7872.2	0.69
4	3128.7	3195.2	2.08	12	8732.6	8559.4	2.02
5	4191.4	4117.7	1.78	13	9011.1	8956.7	0.61
6	4301.5	4324.5	0.53	14	9321.0	9177.1	1.57
7	4847.0	4711.5	2.88	15	9879.4	9760.0	1.22
8	5832.1	5785.3	0.81	16	9939.9	10,012.5	0.72

Table 3. The first four mode shapes.

| No.	1	2	3	4
Mode shapes				

should be noted that during the modelling process, some geometric details on the outer surface of the studied liner were neglected. These details are close to and relevant to the first mode shape of liner. The neglect of geometric details leads to the decrease in the first mode frequency in simulation.

3. Vibration excitations of cylinder liners

According to the engine operation process, combustion shock and piston side-thrust forces are regarded to be two major excitation sources that induce the dynamic responses of cylinder liners. Other possible excitations, such as the ring-induced friction, and lubrication cavitation, are much smaller in amplitudes and not considered in this study.

3.1. Combustion shock

During the premixed combustion period, both the peak pressure and PRR will reach their maximum values and the pressure profile can also accompany with high-frequency oscillations due to unstable combustions. These time-varying pressures are directly applied to the inner surface of the liner, formalizing combustion excitations. To understand the time-frequency characteristics of in-cylinder pressure, a short-time Fourier transform (STFT) result of measured in-cylinder pressure under the operating condition of 1800 rpm engine speed and 40 Nm torque is presented in Figure 4(a). Meanwhile, the raw pressure signal and PRR in Figure 4(b) are also provided to facilitate the analysis of the STFT result.
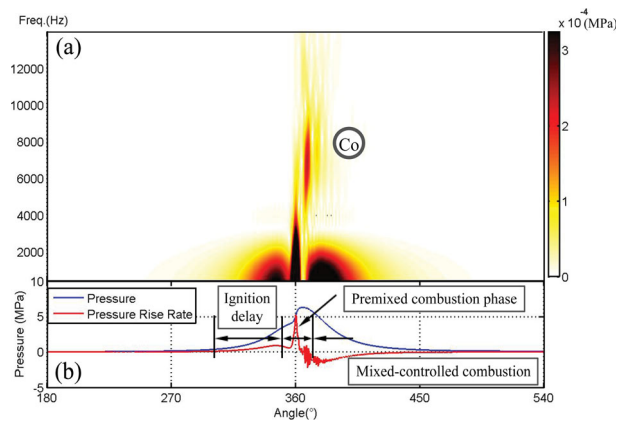
Figure 4. STFT of measured in-cylinder pressure.

It can be seen in Figure 4(a), during the premixed combustion period, there are a series of oscillations can be clearly observed in the frequency range of 4000–8000 Hz immediately after the peak of pressure at a crank angle of about 360°, marked as Ⓒₒ. These pressure oscillations are caused by unstable turbulent movement of gas in the combustion chamber and special inhomogeneity of combustion (Wei, Wei, & Shu, 2012). Moreover, it falls in the range of mode frequencies and thereby induces high-frequency responses on the liner correspondingly.

3.2. Piston side thrust

In addition to this direct excitation of combustion pressure oscillations, the combustion force also drives the piston to move laterally and impact the liner due to the kinetic motion of the piston-connecting rod mechanism.
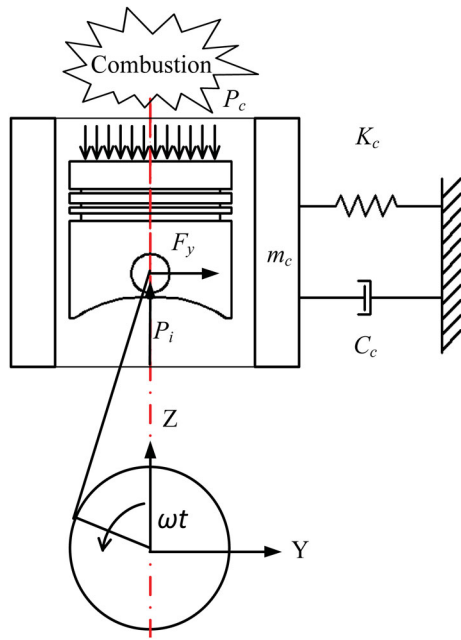
Figure 5. Dynamic model of cylinder assembly.

Figure 6. Composition of the piston lateral force.

As shown in Figure 5, the side-thrust is decomposed from the longitudinally acting combustion force and inertial force of the moving piston assembly, which pushes the piston assembly from one side of the cylinder wall skipping onto the other side, so as to induce an unceasing slap impact on the cylinder wall (Geng & Chen, 2005).

Mathematically, this side-thrust force F_y can be calculated by

$$
\begin{aligned}
F_y &= (P_c - P_i)\lambda \sin \omega t / \sqrt{1 + (\lambda \sin \omega t)^2} \\
&= P_c \times \lambda \sin \omega t / \sqrt{1 + (\lambda \sin \omega t)^2} \\
&\quad + P_i \times \lambda \sin \omega t / \sqrt{1 + (\lambda \sin \omega t)^2} \\
&= F_c - F_i,
\end{aligned}
\tag{1}
$$

where $\lambda = r_c/l$, r_c is the crank radius and l is the length of the connecting rod. The m_l is the equivalent mass of the piston assembly. Figure 6 shows a typical characteristic of the side-thrust force, obtained based on the engine in this study.

The combined side-thrust force F_y every time passes zero and changes direction (from positive to negative, or vice versa) means an possible occurrence of piston slap impact on a definite position along the cylinder wall. In this instance, there are six slap impacts occurring in the four-stroke working cycle which are denoted as Impact Ⓐ0–Ⓕ0, respectively, as illustrated in Figure 6. As Dolatabadi et al. (2015) pointed out, based on the sign change of piston lateral force, six events should be distributed across the four engine strokes, following a
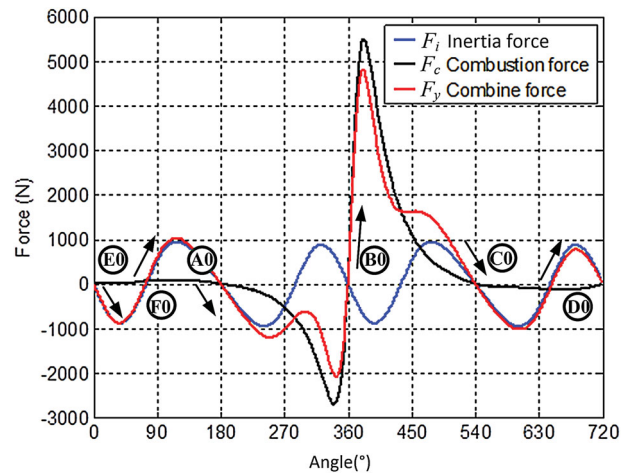
pattern of 3, 0, 2 and 1 events (starting at the intake stroke and ending with the exhaust stroke). Obviously, the force amplitude of Impact Ⓑ0 occurring around the power TDC at 360° is the most significant one. It will results in a higher impact and appears in the similar angular positions to the combustion shock, making it difficult to separate these two effects in measured responses.

4. Numerical evaluation

To gain an understanding of vibrations responses upon the two excitations, a numerical analysis was carried out based on the model under an input of either the combustion force or piston slap force. Figure 7 presents two typical responses respective to the combustion shock and piston slap, at a crank angle of 370°, under the same operating condition of 1800 rpm and 40 Nm.

It can be seen in Figure 7(a) that the significant deformation response to combustion shock is mainly appeared and concentrated in the top portion of the liner, while the response to piston slap extended throughout the liner structure, as seen in Figure 7(b). After removing translation movement and quasi-static deformations, especially that of Figure 7(b), the magnitude information of high-frequency local deformations can be obtained. The predicted amplitude of local responses is in the order of 0.02 microns due to the combustion shock, which may be negligible in predicting lubrications between the piston ring and the liner as it far less than the roughness magnitudes of the lubricated surfaces. However, piston slaps can lead to deformation as high as 0.1 micron, being about 20% of roughness amplitude. Therefore, it needs to be taken into account in analysing the lubrication conditions.

To understand more the difference of dynamic responses between the combustion shock and the piston thrust slap, only examined is the radial displacement
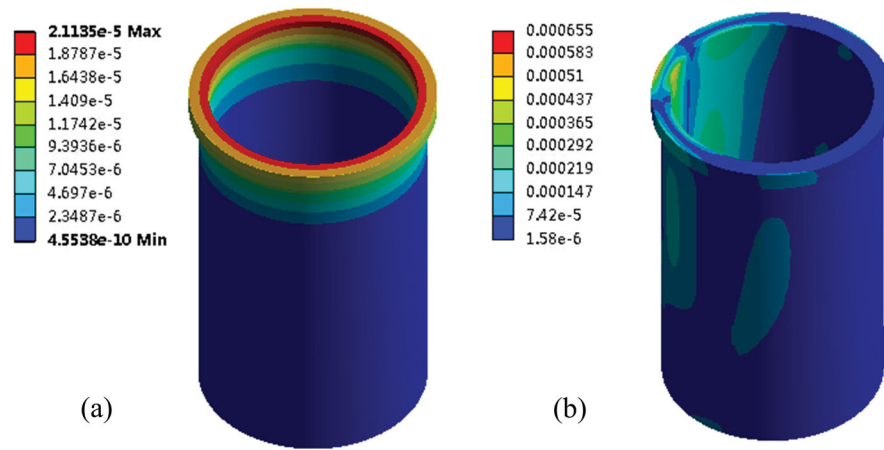
Figure 7. Total deformation of cylinder liner (Unit: mm). (a) Response to combustion shock (b) Response to piston slap.
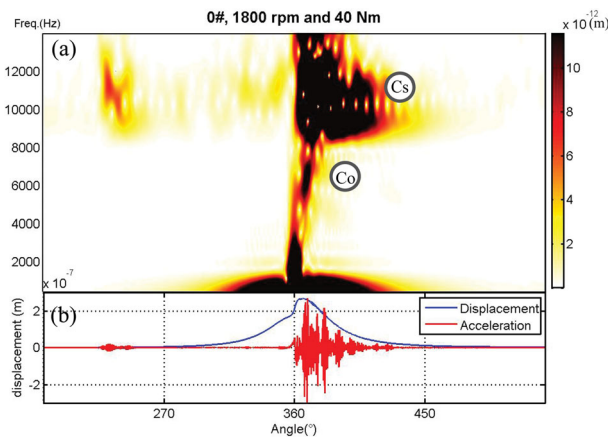

Figure 8. STFT of predicted displacement response to combustion under 40 Nm and 1800 rpm.

response at the node on the anti-thrust side of liner outer surface in order to correspond to the measured results. In addition, the STFT analysis is used to highlight the time-frequency characteristics of the clean prediction, rather than the wavelet analysis used for the noisy measurements.

4.1. Dynamic responses to combustion forces

Figure 8 shows the predicted responses to the pressure force measured from the test engine, detailed in Section 5.1, fuelled with standard diesel under an operating condition of 1800 rpm speed and 40 Nm torque output. It can be seen in Figure 8(b) that the predicted displacement response shows a profile close to the combustion pressure. The significant responses appear around the combustion TDC. In addition to the quasi-static response, there clearly exist series of high-frequency responses sustained for a relative long duration, which are more obvious in the predicted acceleration responses. As seen in Figure 8(a), after the combustion TDC,

there is a significant dynamic response event located in the frequency range of 5000–8000 Hz, marked as Ⓒ₀. As the frequency location and attenuation pattern show a high similarity to the combustion oscillations shown in Figure 4(a), this event is primarily the forced response caused by high-frequency oscillations of in-cylinder pressure.

Moreover, clear oscillating components can be observed in the frequency band of 8000–12,000 Hz, denoted marked as Ⓒₛ. It starts at about 365°, immediately after the peak of the combustion pressure. As there is no such frequency contents in the pressure profile and the oscillation sustains for a long period, which exists even when the input pressure is very low, it is regarded as the modal responses of the liner. A further examination has found that the frequency band is close to 8559–10,012 Hz of the 8th–12th modes identified by the modal experiment, as given in Table 2.

The simulation result indicates that in-cylinder combustion process can activate high-frequency modal responses of liner structure, which might be attributed to the rapid rise rate of pressure during the premixed combustion period.

As shown in Figure 9(c) and (d), under the low-speed conditions, sustained angular of dynamic responses excited by combustion pressure is shorter than that of high-speed conditions, and more concentrated in frequency band of 6 and 10 kHz. In high-speed conditions, the sustained angular of responses can be extended to 40–60 degrees. The dynamic response moves to higher frequency band of 8 and 12 kHz, and contains more high-order modal components, indicating that sharper and faster combustion pressure is prone to activate more high-frequency modal responses. As the load increases, these trends are more pronounced.

After being processed by high-pass filter, a preliminary study on the amplitude of dynamic deformations has
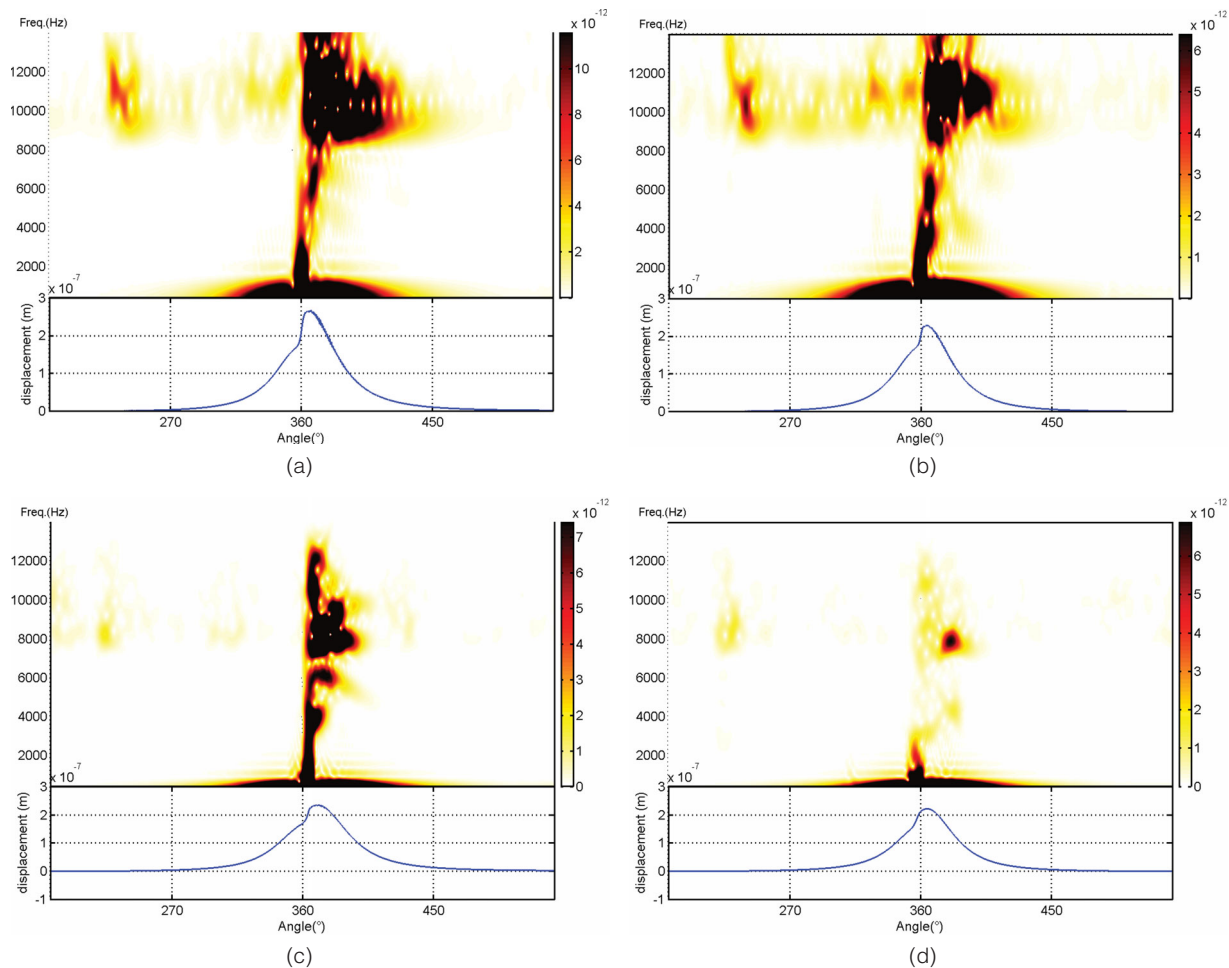
Figure 9. STFT of predicted displacement response to combustion shocks (Unit: m). (a) 1800 rpm and 40 Nm, max. amplitude: 0.015 μm. (b) 1800 rpm and 10 Nm, max. amplitude: 0.01 μm. (c) 1000 rpm and 40 Nm, max. amplitude: 0.005 μm. (d) 1000 rpm and 10 Nm, max. amplitude: 0.004 μm.

been carried out. With the increase in operating speed and load, the deformation magnitude of measuring node increased from 0.004 to 0.015 microns. The predicted amplitude of local responses is less than 3% of the surface roughness amplitude, which may be negligible to affect lubrications.

4.2. Dynamic responses to piston slaps

In the case of piston lateral slap being considered alone, the dynamic response of the liner at corresponding measuring point shows more complex and abundant patterns in STFT results, as shown in Figure 10(a), which corresponds to the piston side-thrust force in Figure 10(b) obtained under the operating condition of 1800 rpm and 40 Nm. In Figure 10(a), six distinctive transient responses can be clearly observed corresponding to the peaks and troughs of piston side-thrust force, which are marked by Ⓐ–Ⓕ. Obviously, these responses mainly appear at the first three modes, especially for the responses to the slaps

away from combustion. The fourth modal response can only be observed around the combustion event.

Moreover, three more dynamic events, marked as Ⓖ, Ⓗ and Ⓘ, can also be observed in Figure 10(a). These events correspond to the secondary impact events induced by sustained high-amplitude side-thrust force, rather than by any particular force peak or trough, showing that the sustained high-amplitude side-thrust force may also cause additional impacts.

Previous studies (Badaoui et al., 2005; Dolatabadi et al., 2015; Geng & Chen, 2005; Servière et al., 2005) tend to select a common frequency range of 500–3000 Hz, as a rule of thumb, for the detection and analysis of piston slap events. As shown in Figure 10, the distribution of dynamic responses in the frequency domain shows that the experience-based selection of frequency domain has certain rationality. The origins of this rationality may lie in the inherent mode characteristics of liner structures. As illustrated in the simulation of this study, the dynamic responses excited by piston slaps are mainly
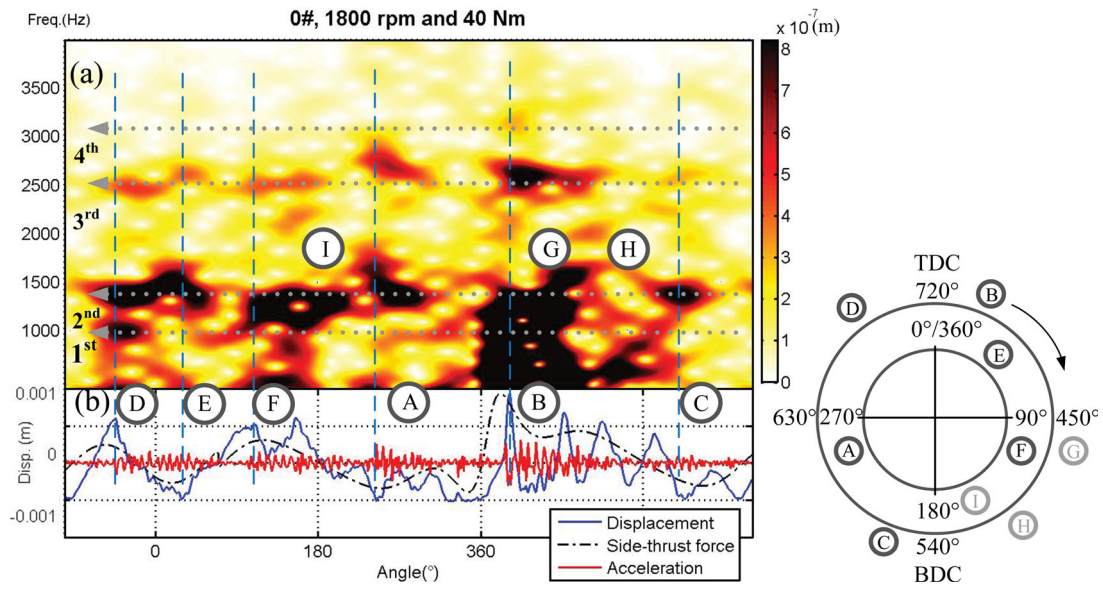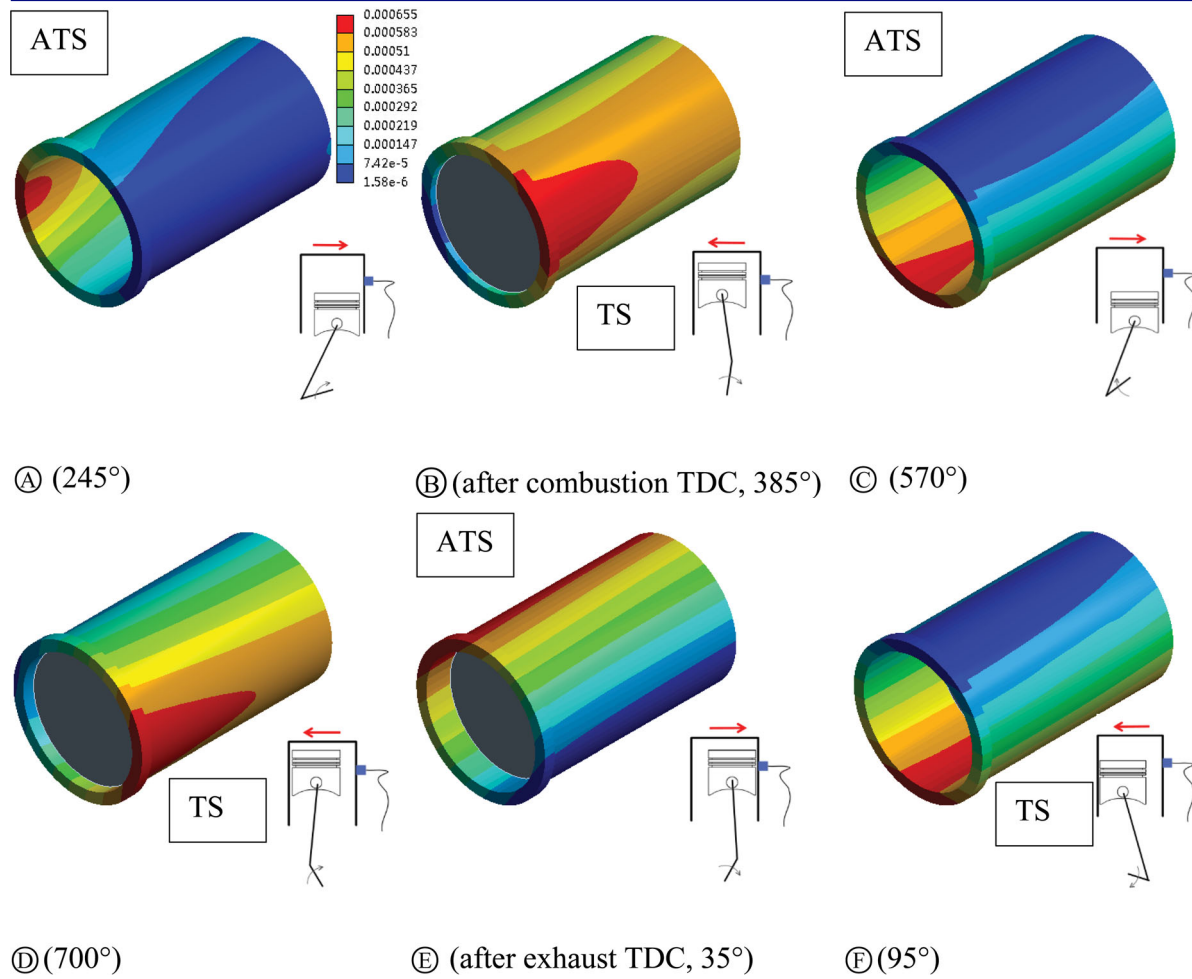
Figure 10. STFT of responses to piston slaps under 40 Nm and 1800 Nm.

Table 4. Deformations caused by slap events at different angular positions (Unit: mm).

Ⓐ (245°)   Ⓑ (after combustion TDC, 385°)   Ⓒ (570°)

Ⓓ (700°)   Ⓔ (after exhaust TDC, 35°)   Ⓕ (95°)

concentrated in the frequency range of 600–3500 Hz, being close to the frequency band of the first four modes. It means that the dynamic responses of cylinder liners may be highly relevant to their structural modes.

Dolatabadi et al. (2015) suggested that, based on the sign change of piston lateral force, six events should be distributed across the four engine strokes, following a pattern of 3, 0, 2 and 1 events (starting at the intake stroke and ending with the exhaust stroke), as seen in Figure 6. However, the simulated events caused by sign changes of piston lateral force show a different pattern of 2, 1, 1 and 2 events over the four engine strokes. With the addition of events Ⓖ, Ⓗ and Ⓘ, the distribution pattern of slap events eventually becomes even 3, 1, 2 and 2. This indicates that the sign changes cannot well characterize the occurrence of slap events.

It is true that change of sign in driving force does lead to the occurrence of the piston slap, but as to the timing of occurrence, more practical factors such as the clearance, surface stiffness, geometric shapes and material properties, are required to in-depth understand the impact process. It demonstrates again the necessity and rationality of the selection of FEA method in dynamics modelling for this study.

It should be noted that, the slap-induced events appeared at different angular positions show significant differences in both frequency components and patterns. The main causes of these variations are varying impact position and unilateral measuring method.

As seen in Figure 10, the differences existed in degree and patterns of slap-induced responses at different angular positions cannot be well interpreted by differences in magnitude of side-thrust force. For example, there is not much difference in the amplitude of three peaks Ⓓ, Ⓔ and Ⓕ from 630° to 720°, then to 180° of next cycle, while their dynamic responses show great differences in frequency characteristic. To fully understand the causes, dynamic deformations of cylinder liner at each slap moment have been selected and organized, as given in Table 4.

(1) The frequency range of dynamic responses excited by piston slaps is highly relevant to the slap position, that is, the location of collision occurred. When the
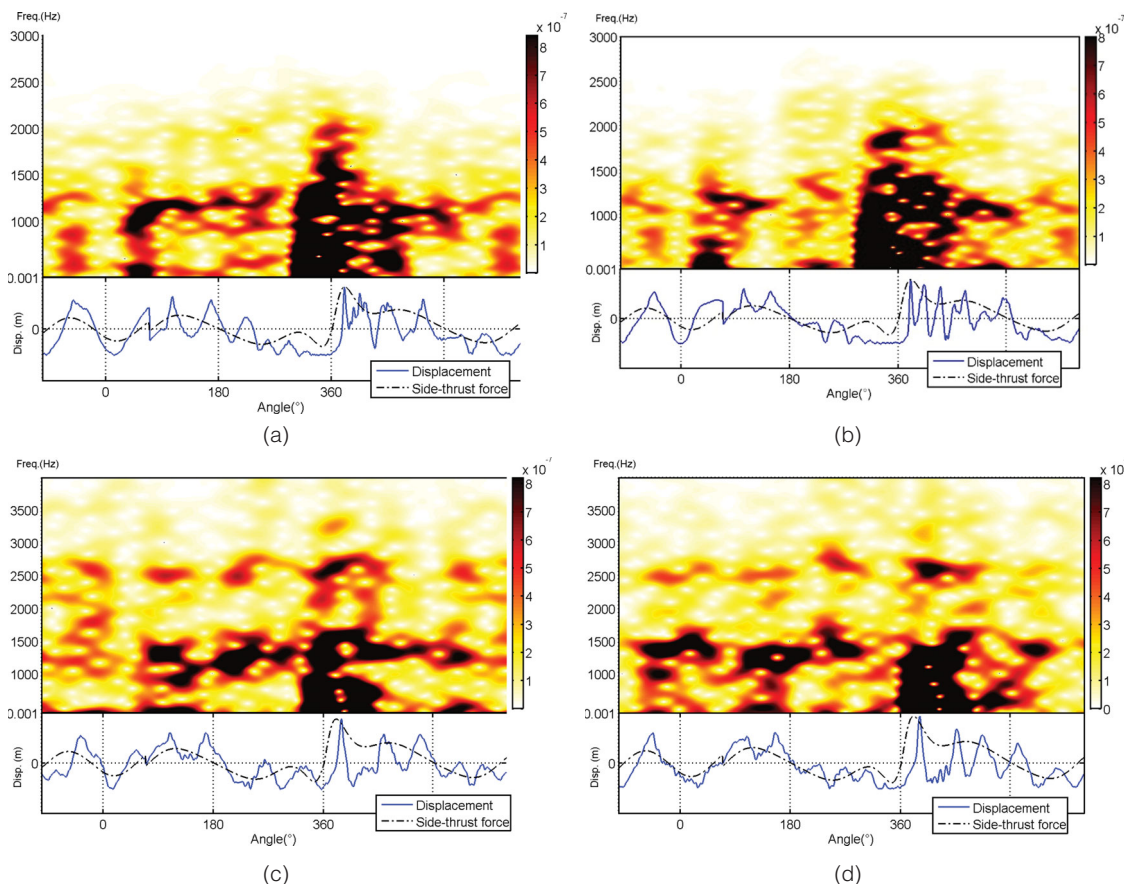

Figure 11. The STFT of dynamic displacements at different operating conditions (Unit: metre). (a) 1000 rpm and 10 Nm, magnitude = 0.02–0.10 μm. (b) 1000 rpm and 40 Nm, magnitude = 0.02–0.10 μm. (c) 1800 rpm and 10 Nm, magnitude = 0.04–0.15 μm. (d) 1800 rpm and 40 Nm, magnitude = 0.04–0.15 μm.

slap position is close to the deformation region of a mode shape, the slap event is prone to excite more frequency components related to this mode. When piston slap occurred near the top flange of liner, the deformation trend of cylinder liner is close to the modal shape of the second mode, as given in Table 3. This explains why the slap-induced events, Ⓑ, Ⓓ and Ⓔ, show more intense second-order modal features than the others. In contrast, when the slap position move down to the bottom end of cylinder liner, cylinder wall will show a deformation trend similar to the first- and third-order modal shapes, as Ⓐ and Ⓕ events seen in Figure 10.

As seen in Figure 10 and Table 4, although the slap position is close to the lower part of cylinder liner, the deformation of liner at event Ⓒ shows more second-order modal features rather than the first- or third-order modal response. The most probable reason of this phenomenon is that at this moment the piston exactly knocks at the bottom portion of liner where it is surrounded by the lower edge of the water jacket. It is similar to the situation of knock occurs at a stationary point in harmonic vibrations, that most of odd-order modal responses have been suppressed in this case.

(1) When piston slap occurs at different sides of cylinder liner, that is, the thrust side and anti-thrust side, the dynamic responses measured at the same measuring point will present obvious differences in the modal components. When the measuring point is located at the deformation region of a mode shape, the response frequency of this mode is much easier to be measured. As shown in Figure 10, the deformations of liner at different moments of Ⓐ, Ⓒ and Ⓔ show more second-order modal features than the other modal components.
(2) The number of observable slap-induced events does not only depend on the number of sign changes but also on the contact parameters and piston movement parameters. As it can be seen from Figure 10, after the combustion TDC, in addition to dynamic event Ⓑ, there are two weaker dynamic events that can be observed from 450° to 495°, which can well correspond to the peaks of piston lateral displacement in Figure 10(b). Once the impact Ⓑ occurred, in the process of leaving from liner surface, the piston was pulled back to the liner surface again by the sustained high-amplitude side-thrust force, leading to secondary slap events.

As seen in Figure 11(a) and (b), under the low-speed conditions, there are only two major dynamic events

could be observed around the combustion TDC and exhaust TDC separately. With the increase in operating speed and load, there are more dynamic events appeared on the time-frequency spectrum of dynamic responses, accompanied by more high-frequency modal components.

5. Experimental verification

5.1. Experimental set-up

To verify the numerical predictions, experimental studies were made based on a single-cylinder diesel engine, as given in Table 5. An accelerometer for measuring liner vibrations is installed directly on the external surface of the liner through a waterproof adapter. In addition, in-cylinder pressure, engine speed and time-based crank angle are also recorded for both the FEM calculations and results calibrations. The experimental set-up is illustrated in Figure 12. All the data were recorded simultaneously by a multiple channel acquisition system, and thereafter processed offline for making corresponding comparisons against FEM predictions.

Table 5. Specification of the test engine.

Manufacturer	Quanjiao Power Co., Ltd., PR. China
Engine type	QCH1110
Number of cylinders	One
Combustion system	Direct injection, toroidal combustion Chamber
Bore/stroke	110/115 mm
Displacement volume	1.093 L
Compression ratio	18:1
Cylinder liners	Cast iron replaceable wet liner
Start of fuel injection	$14 \pm 2°$ BTDC
Rated power	14.7/2400 kW/r/min
Piston clearance	0.5 mm

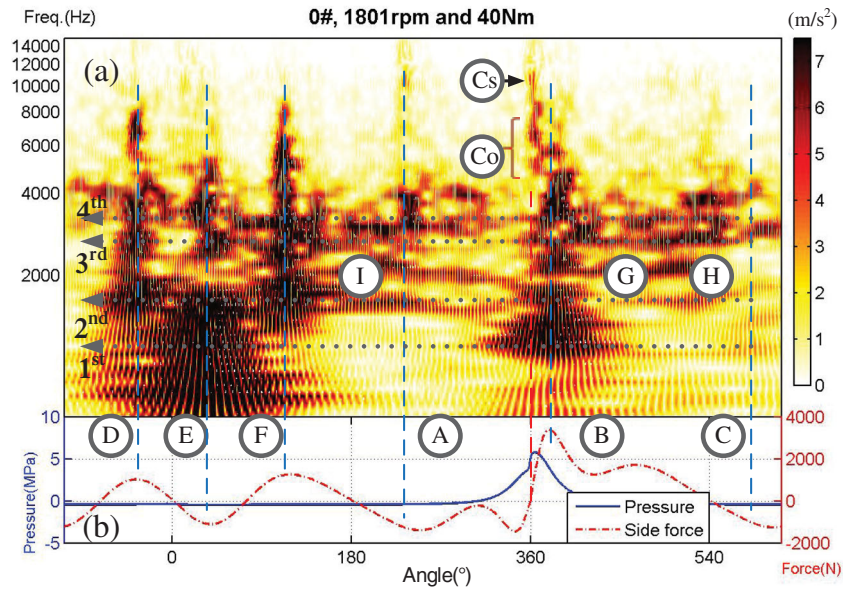**Figure 12.** A photograph of the diesel engine test rig.

Figure 13. CWT of vibration signal under 40 Nm and 1800 rpm.

5.2. Diagnostic analysis

As the measured vibration contains random noise and exhibits high non-stationarity, continuous wavelet transform (CWT) was applied to the raw vibration to highlight the dynamic responses localized in the joint time and frequency domains. In addition, the wavelet result was averaged over 80 engine cycles to further suppress noise and random short duration interferences for obtaining reliable results.

Figure 13 presents a typical CWT result of the liner vibration under the operating condition of 1800 rpm and 40 Nm. The complicated time-frequency characteristics in Figure 13(a) can be viewed as having the following key patterns.

The significant responses, marked as Co and Cs appear around the combustion TDC at 360° and in the frequency range from 6000 to 8000 Hz, and 8000 to 12,000 Hz. Moreover, they can well correspond to the peak of in-cylinder
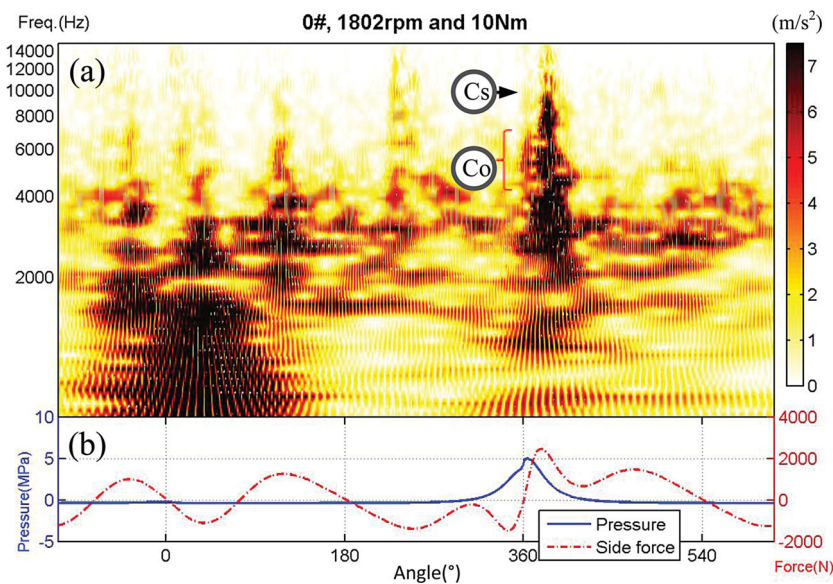

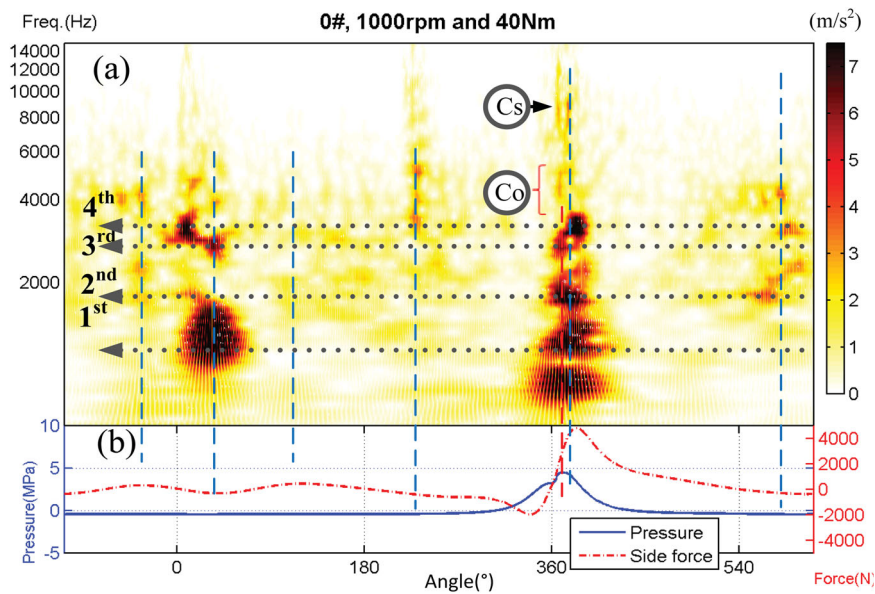**Figure 14.** CWT of vibration signal under 10 Nm and 1800 rpm.

Figure 15. CWT of vibration signal at 40 Nm and 1000 rpm.

pressure, which is agreeable with the numerical prediction presented in Section 4.1 and Figure 8.

More distinctive responses, marked as Ⓐ to Ⓕ, correspond to dynamic events induced by piston slaps, being consistent with that in Section 4.2 and Figure 10. These responses appear in the frequency band from 900 to 4000 Hz, which associates with the first four modal frequencies of the cylinder liner.

Furthermore, three more events predicted in dynamic simulation can also be observed in Figure 13(a), marked as Ⓖ, Ⓗ and Ⓘ in the frequency range around 2000 Hz, showing that the sustained high-amplitude side-thrust force can cause repeated impacts, which agrees with that of the established FEM.

Likewise, the time-frequency responses of the liner under a lower load show significant patterns corresponding to the combustion shock which is marked as Ⓒs in Figure 14. However, the combustion is smoother when they are in a frequency band from 6000 to 10,000 Hz, which is 2000 Hz lower than that of higher load. Moreover, almost all of the slap-induced events above 2000 Hz are significantly reduced, showing that the piston movement driven by the smoother combustion is prone to exciting more low-frequency mode components.

At the low-speed of 1000 rpm and 40 Nm, CWT plots in Figure 15(a) show significant reduction of amplitudes for all dynamic events aforementioned. Particularly, only two events around the combustion TDC and exhaust TDC are still significant. The main reason is that, under low-speed conditions, the kinetic energy of the piston lateral movement is low due to the reduced reciprocating inertia force, which leads to a reduction in the frequency content of the piston side-thrust force.

6. Conclusions

Based on the comparison between FEM prediction and experimental evaluation in the time-frequency domain, it can be concluded that developed FEM is acceptable, as it provides vibration responses agreeable with measurements. Particularly, the dynamic responses of cylinder liners to combustion excitation appear in higher frequency modes from 4 to 12k Hz; whereas that of piston impacts are in lower frequency modes from 1 to 4 kHz. Moreover, the responses exhibit short-time impulses and are well associated with engine operating strokes. Therefore, they allow correct diagnosis of different vibration sources. Furthermore, the predicted amplitude of local responses is at the order of 0.01 microns due to combustion, which may be negligible to affect lubrications. However, piston slaps can lead to deformation as high as 0.1 microns, being about 20% of roughness amplitude. Consequently, its effect on lubrication performance, friction losses and wear rate of liners will be investigated further. To study the impact of higher frequency dynamic deformations on the tribological behaviours between the piston rings and cylinder liners, it is necessary to further increase the simulation steps and to reduce the mesh size to obtain higher frequency and more refined surface deformation predictions, which may require the support of high-performance computing systems in future research.

Disclosure statement

No potential conflict of interest was reported by the authors.

Funding

References

Badaoui, M. E., Danière, J., Guillet, F., & Servière, C. (2005). Separation of combustion noise and piston-slap in diesel engine – part I: Separation of combustion noise and piston-slap in diesel engine by cyclic wiener filtering. *Mechanical Systems and Signal Processing*, *19*(6), 1209–1217. doi:10.1016/j.ymssp.2005.08.010

Cho, J. R., & Moon, S. J. (2005). A numerical analysis of the inter-action between the piston oil film and the component deformation in a reciprocating compressor. *Tribology International*, *38*(5), 459–468. doi:10.1016/j.triboint.2004.10.002

Dolatabadi, N., Theodossiades, S., & Rothberg, S. J. (2015). On the identification of piston slap events in internal combustion engines using tribodynamic analysis. *Mechanical Systems and Signal Processing*, *58–59*, 308–324. doi:10.1016/j.ymssp.2014.11.012

Farshidianfar, A., Farshidianfar, M. H., Crocker, M. J., & Smith, W. O. (2011). Vibration analysis of long cylindrical shells using acoustical excitation. *Journal of Sound and Vibration*, *330*(14), 3381–3399. doi:10.1016/j.jsv.2011.02.002

Geng, Z., & Chen, J. (2005). Investigation into piston-slap-induced vibration for engine condition simulation and monitoring. *Journal of Sound and Vibration*, *282*(3–5), 735–751. doi:10.1016/j.jsv.2004.03.057

Hiroshi, K., Okubo, M., & Yonezawa, T. (1990). *Analysis of noise sources and their transfer paths in diesel engines* (SAE Technical Paper No. 900014). Warrendale, PA: SAE Technical Paper. Retrieved from http://papers.sae.org/900014/

Jafari, A. A., Khalili, S. M. R., & Azarafza, R. (2005). Transient dynamic response of composite circular cylindrical shells under radial impulse load and axial compressive loads. *Thin-Walled Structures*, *43*(11), 1763–1786. doi:10.1016/j.tws.2005.06.009

Liu, X., & Randall, R. B. (2005). Blind source separation of internal combustion engine piston slap from other measured vibration signals. *Mechanical Systems and Signal Processing*, *19*(6), 1196–1208. doi:10.1016/j.ymssp.2005.08.004

Murakami, H., Nakanishi, N., Ono, N., & Kawano, T. (2011). *New three-dimensional piston secondary motion analysis method coupling structure analysis and multi body dynamics analysis* (SAE Technical Paper No. 2011-32–0559). Warrendale, PA: SAE International. Retrieved from http://papers.sae.org/2011-32-0559/

Servière, C., Lacoume, J.-L., & El Badaoui, M. (2005). Separation of combustion noise and piston-slap in diesel engine – part II: Separation of combustion noise and piston-slap using blind source separation methods. *Mechanical Systems and Signal Processing*, *19*(6), 1218–1229. doi:10.1016/j.ymssp.2005.08.026

Wang, E., & Nelson, T. (2002). Structural dynamic capabilities of ANSYS. In ANSYS 2002 Conference, Pittsburg, Pennsylvania, USA. Retrieved from http://www.designspace.com/staticassets/ANSYS/staticassets/resourcelibrary/confpaper/2002-Int-ANSYS-Conf-200.PDF

Wei, H., Wei, J., & Shu, G. (2012). Calculation on cylinder pressure fluctuation by using the wave equation in KIVA program. *Chinese Journal of Mechanical Engineering*, *25*(2), 362–369. doi:10.3901/CJME.2012.02.362